



ORIGINAL ARTICLE

Electrochemical degradation of methylene blue dye using a graphite doped PbO₂ anode: Optimization of operational parameters, degradation pathway and improving the biodegradability of textile wastewater



Mohammad Reza Samarghandi^a, Abdollah Dargahi^{b,c,*}, Amir Shabanloo^{d,*}, Hassan Zolghadr Nasab^e, Yaser Vaziri^e, Amin Ansari^f

^a Research Center for Health Sciences and Department of Environmental Health Engineering School of Public Health, Hamadan University of Medical Sciences, Hamadan, Iran

^b Department of Environmental Health Engineering, School of Health, Ardabil University of Medical Sciences, Ardabil, Iran

^c Social Determinants of Health Research Center, School of Health, Ardabil University of Medical Sciences, Ardabil, Iran

^d Student Research Committee, Department of Environmental Health Engineering, Hamadan University of Medical Sciences, Hamadan, Iran

^e Department of Environmental Health Engineering, School of Public Health, Hamadan University of Medical Sciences, Hamadan, Iran

^f Faculty of Chemistry, Bu-Ali-Sina University, Hamadan, Iran

Received 19 May 2020; accepted 30 June 2020

Available online 9 July 2020

KEYWORDS

Anodic oxidation;
Biodegradability index;
Graphite anode;
Lead dioxide;
Textile wastewater

Abstract An anodic oxidation process with graphite anode coated with lead dioxide (G/ β -PbO₂) was optimized for the degradation of methylene blue (MB) and the treatment of real textile wastewater. The G/ β -PbO₂ anode was prepared by the electrochemical precipitation method. The scanning electron microscopy (SEM), energy-dispersive X-ray spectroscopy (EDX), and X-ray diffraction (XRD) analyses confirmed the successful coating of graphite substrate with the β -PbO₂ film. The effect of four independent variables including pH, reaction time, current density, and electrolyte concentration of Na₂SO₄ on the performance of the electrochemical oxidation system was modeled by using a complete central composite design and was then optimized by genetic algorithm method.

* Corresponding authors at: Department of Environmental Health Engineering, School of Health, Ardabil University of Medical Sciences, Ardabil, Iran (A. Dargahi).

E-mail addresses: a.dargahi29@yahoo.com (A. Dargahi), shabanlo_a@yahoo.com (A. Shabanloo).

Peer review under responsibility of King Saud University.



Production and hosting by Elsevier

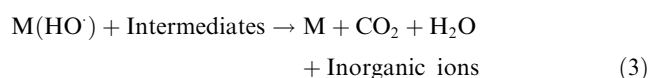
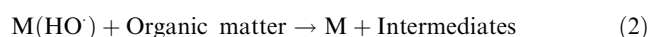
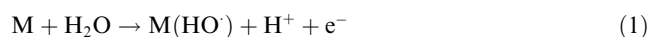
The accuracy of the proposed quadratic model by CCD was confirmed with p -value < 0.0001 and $\text{adj-R}^2 > 0.9$. The optimum conditions for solution pH, reaction time, current density, and Na_2SO_4 electrolyte concentration were obtained to be 5.75, 50 min, 10 mA/cm^2 , and 78.8 mg/L , respectively. In these conditions, the experimental removal efficiencies of MB using G/ β - PbO_2 and graphite anodes were 96.2% and 68.3%, respectively. The electrochemical removal of MB using both G/ β - PbO_2 and graphite anodes well followed the pseudo-first-order reaction ($\text{R}^2 > 0.9$). Cyclohexane, cyclohexa-2,5-dien-1-ylum, and N-(*sec*-butyl) aniline were the most abundant intermediates identified by LC-MS analysis. However, the complete mineralization of MB was achieved in 60 min. The optimized anodic oxidation process successfully improved the biodegradability of real textile wastewater ($\text{BOD}/\text{COD} > 0.4$).

© 2020 The Author(s). Published by Elsevier B.V. on behalf of King Saud University. This is an open access article under the CC BY-NC-ND license (<http://creativecommons.org/licenses/by-nc-nd/4.0/>).

1. Introduction

Pollution of water resources by wastewater containing synthetic color compounds, especially in the textile industry, is a major environmental concern (Shokoohi et al., 2020). Today, more than 100,000 types of commercial dyes have an annual production rate of about 700,000 tons (Yang et al., 2017). Of these, approximately 15% of the dye compounds used in industry enter the effluent during the production and processing stages and are eventually discharged into the environment (Gupta et al., 2012). Most of the colorful compounds, as well as the intermediates produced by their degradation, are considered as a major health hazard for the human environment and other organisms, especially aquatic life. Methylene blue (MB) is classified in the cationic dye group (Alver et al., 2020), which is used in various applications including chemistry, biology, medical sciences, and dyeing. Long-term exposure to this dye leads to vomiting, nausea, anemia, and hypertension (Pathania et al., 2017). Various methods, e.g., advanced oxidation processes (Asgari et al., 2020; Samarghandi et al., 2020), adsorption (Yao et al., 2020), electro-coagulation (Golder et al., 2005), ozonation (Zhang et al., 2009), membrane separation (Jua et al., 2020), and biological treatment (Paz et al., 2017) have been studied for degradation of dye compounds. The advantages and disadvantages of each of these methods have been detailed in studies (Gupta, 2009; Rahmani et al., 2016; Seid-Mohammadi et al., 2017). Electrochemical advanced oxidation processes (EAOPs) are capable of degrading organic materials to CO_2 and H_2O through reaction with hydroxyl radicals (HO^\cdot) (Martínez-Huitle et al., 2015; Yao et al., 2019a). The simplicity of equipment and easy operation, low cost of construction, no sludge generation, mineralization of pollutants, and advancing reaction by electron are among the advantages of EAOP (Rahmani et al., 2015; Stirling et al., 2020). In EAOP/anodic oxidation (AO), organic pollutants are degraded by both direct and indirect oxidation. In direct oxidation, electrons are transferred from the organic pollutant to the anode surface. In indirect oxidation, the electroactive species produced in the solution act as mediators for pollutant degradation (Martínez-Huitle and Panizza, 2018; Panizza and Cerisola, 2009). Research demonstrates that the main mechanism of indirect oxidation is the mineralization of organic matter with HO^\cdot (Anglada et al., 2009; Mandal et al., 2018). As shown in Eq. (1), H_2O is first discharged at the anode surface (M) to form HO^\cdot . Then according to Eqs. (2) and (3), organics are oxidized by adsorbed hydroxyl

radicals $\text{M}(\text{HO}^\cdot)$ to complete mineralization (Brillas and Martínez-Huitle, 2015; Souri et al., 2020).



Although the type of contaminant, reaction time, type and concentration of electrolyte, current density, etc. are among the operational parameters affecting the efficiency of electrochemical oxidation processes, the anode material plays the most important role in the performance of AO processes (Rao and Venkatarangaiah, 2014; Wu et al., 2014). Based on the interactions of produced HO^\cdot radical with the surface of the anode, the anodes are classified into two groups, i.e., the active anode and the non-active anode. Active anodes have low oxygen evolution potential and lead to incomplete oxidation of organic pollutants. However, non-active anodes have high oxygen evolution potential and the organic compound can be completely mineralized to H_2O and CO_2 . Ruthenium dioxide (RuO_2), iridium dioxide (IrO_2), platinum (Pt), graphite, and other sp^2 carbon-based electrodes are the most popular active anodes. Lead dioxide (PbO_2), tin dioxide (SnO_2), boron-coated diamond (BDD), and non-stoichiometric TiO_2 electrodes are classified as non-active anodes (Panizza and Cerisola, 2009). The BDD anode has the highest oxygen evolution potential and stability among the non-active anodes. However, its high cost is a major constraint (Ciriacio et al., 2009). In this regard, metal oxide-coated substrates can be a suitable alternative for wastewater treatment (Rao and Venkatarangaiah, 2014; Wu et al., 2014). Antimony-doped SnO_2 (Sb-doped SnO_2) due to its high ability to produce HO^\cdot is a good choice. However, the short service life is the main limitation of this anode (Song et al., 2010). PbO_2 electrode as a non-active anode has shown good properties, which are: excellent electrocatalytic performance, long service lifetime, low cost and ease of preparation, good chemical stability, high oxygen evolution potential, and high conductivity (Panizza and Cerisola, 2009; Yao et al., 2019b). Various substrates, such as stainless steel, titanium, lead, and graphite, have been used to fabricate the PbO_2 anode (Ansari and Nematollahi, 2018). Titanium has been widely studied due to its high stability and good conductivity. However, high cost and inactivation due to the formation of TiO_2 in the presence

of oxygen are major disadvantages of titanium substrates (Mandal et al., 2018). As a viable alternative, graphite substrates (G) have been used successfully to fabricate PbO₂ anodes (Mandal et al., 2020). PbO₂ anodes have been widely used to degrade a variety of organic pollutants. However, few studies have investigated the ability of these anodes to treat industrial wastewater. This is a major gap in the commercialization and industrialization of EAOP-based treatment methods (Garcia-Segura et al., 2020). Industrial wastewater pretreatment with an EAOP-based treatment system is able to effectively improve the biodegradability of wastewater by degrading toxic pollutants (Soloman et al., 2009). Also, in most studies, only the linear effects of operational variables on system performance have been investigated, and the interactive and quadratic effects have not been identified. Central composite design (CCD) and genetic algorithm (GA) are two effective tools for optimizing water and wastewater treatment systems (Asgari et al., 2020; Samarghandi et al., 2020; Shabanloo et al., 2020; Shokoohi et al., 2019). Using these techniques, a multivariate process can be optimized with a limited number of experiments.

Based on the literature review, no study has been conducted to investigate the ability of G/β-PbO₂ in improving the biodegradability of textile wastewater. In this study, MB dye was selected as the model pollutant, and after optimizing the process, the performance of the G/β-PbO₂ anode was investigated for improving the biodegradability of textile wastewater released from the local textile industry. For this purpose, G/β-PbO₂ anode was prepared by the electrodeposition method, and after the characterization of structural and morphological properties, its ability to degrade MB dye was investigated. The effect of four independent variables including solution pH, reaction time, current density, and Na₂SO₄ concentration on MB dye removal efficiency was optimized using CCD and GA methods. In addition, under optimal operating conditions, the intermediates caused by MB degradation was identified and a path was proposed for its mineralization.

2. Materials and methods

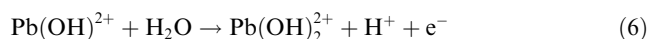
2.1. Chemicals

Methylene blue (≥97%), lead nitrate (≥99%), nitric acid (≥90%), sodium sulfate (≥99%), sodium hydroxide pellets (≥98%) and sulfuric acid (≥98%) were purchased from Merck company. The graphite substrates were purchased from Atlas Equipment Company (Iran). All chemical reagents used in this study were of analytical grade and used without further purification.

2.2. Preparation and characterization of G/β-PbO₂ anode

The electrochemical precipitation method was used to prepare G/β-PbO₂ anode. Firstly, the graphite plates (dimensions of 10 cm × 3 cm × 0.2 cm) were polished by fine grade sandpaper (400 grid) and then rinsed with deionized water. In the following, the polished graphite plates were sonicated in the 40% NaOH solution and 1:1 (V/V) HNO₃/H₂SO₄ for 60 min. This can be very useful for the stability of the total β-PbO₂ electrodeposited. Finally, the prepared graphite plates were washed several times with deionized water and then transferred

to an electrodeposition constant-current cell. The electrodeposition and constant-current electrolysis were powered by a DC power source (MEGATEK, MP-3005, China). Electrolyte solution containing 500 mL of 0.5 M Pb(NO₃)₂ and 0.1 M HNO₃ (Dargahi et al., 2018). The pre-treated graphite plate was used as the anode and the stainless-steel plate of the same area was used as the cathode. The electrochemical deposition of β-PbO₂ on graphite was carried out under an applied current of 7.5 mA/cm² for 180 min (Ansari and Nematollahi, 2018). After the electrodeposition process, the prepared G/β-PbO₂ was rinsed several times with deionized water (Chen et al., 2016). PbO₂ electrodeposition reactions are as follows (Li et al., 2011):



The average amount of electrodeposited β-PbO₂ on the electrodes surface calculated by Faraday law (Eq. (8)) (Ansari and Nematollahi, 2018; Nasirpour, 2017).

$$W = (I \cdot t \cdot A) / n \cdot F \quad (8)$$

where *w* (g) is the weight of deposit metal, *I* (A) is the current, *t* (s) is the time, *A* (g/mol) is the atomic weight, *n* (equivalents/mol) is the valence of the dissolved metal in solution and *F* is Faraday's constant (96485.309 C/equivalent). Accordingly, the average amount of β-PbO₂ on the electrode surface was 87.0 mg/cm².

Scanning electron microscopy (SEM) analysis along with energy-dispersive X-ray spectroscopy (EDX) (model HITACHI S-4160, Japan) was used to investigate the surface morphology and chemical composition of the prepared G/β-PbO₂ anode. Phase type and crystallite structure of lead dioxide film precipitated on the graphite substrate surface were investigated by X-ray diffraction analysis (Rigaku RINT2200, Japan).

2.3. Electrochemical degradation experiments and analytical methods

All electrochemical degradation experiments were performed in a 250 mL-batch reactor. A stainless steel 316 (SS316) plate with dimensions equal to the G/β-PbO₂ anode was used as the cathode. Two G/β-PbO₂ anodes and a SS316 cathode were placed parallel to the sample solution at a distance of 2 cm from each other. The reactor contents were mixed by a magnetic stirrer at a constant speed of 250 rpm. The schematic of the electrochemical degradation setup is illustrated in Fig. 1. H₂SO₄ and NaOH were used to adjust the pH of the sample solution (pH meter; SensION, HACH). Na₂SO₄ was used as the supporting electrolyte at different concentrations. After adjusting the pH of the solutions containing MB and Na₂SO₄ electrolyte, experiments were conducted galvanostatically with a DC power supply (DAZHENG PS-305D, China). Finally, after the end of the electrochemical degradation reaction, an appropriate aliquot of the reaction solution was taken for analysis. The real wastewater samples were obtained from



Fig. 1 Schematic of the experimental setup (1. SS316 cathode, 2. G/β-PbO₂ anodes, 3. Magnetic stirrer, 4. Magnet, 5. DC power supply).

a local textile industry (Nakh Rang company). Samples were collected before entering the effluent to the wastewater treatment plant. The provided samples were kept in a dark container at 4 °C for a week. The characteristics of raw and treated wastewater are presented in Table 5.

Dye removal was measured by a UV–vis spectrophotometer (DR6000, HACH) at a maximum wavelength of 660 nm (Wu et al., 2017). Chemical oxygen demand (COD) was measured using digestion vials (Ultra-Range COD reagent, Range: 20–1500 mg/L COD, Hack, CO, USA). In this method, 2 mL of the reaction sample was added to the vial and thoroughly mixed with COD reagent. It was then heated in the digestion reactor at 150 °C for 2 h. Finally, the COD of the sample was measured by a spectrophotometer (DR6000, HACH). The biological oxygen demand (BOD₅) of the samples was also measured manometrically with a respirometer (BSB-Controller model 620 T, WTW). An accurate index for defining the biodegradability of effluent is the BOD₅/COD ratio. Accordingly, wastewaters with BOD₅/COD ≥ 0.4 is considered to be biodegradable (Garcia-Segura et al., 2017). MB mineralization was measured by a TOC (Total Organic Carbon) analyzer (Elementar Analysensysteme GmbH, Germany). Intermediate compounds produced during electrochemical oxidation of MB dye were identified by LC-MS analysis (Shimadzu LCMS 2010 A). The cyclic voltammetry experiments were performed at room temperature in a conventional three-electrode one compartment glass cell (Autolab PGSTAT-20 instrument monitored with the Electrochemical System Software (Nova)). The working electrode used in the voltammetry experiments

was a glassy carbon disc (1.8 mm² area). A platinum wire was used as the counter electrode and an Ag/AgCl (3 M) was used as the reference electrode. All of the electrodes were manufactured by AZAR Electrode Company (Urmia, Iran). The concentration of Pb²⁺ in the treated sample was measured by cyclic voltammetry and inductively coupled plasma optical emission spectrometer (ICP-OES, 730 ES, Varian Scientific Instruments). The kinetic of dye removal in the oxidation system was calculated using Eq. (9).

$$\ln\left(\frac{C_t}{C_0}\right) = -k_{\text{obs}} \times t \quad (9)$$

where C₀ and C_t are MB dye concentrations at time zero and time t of the electrochemical degradation reaction, respectively. k_{obs} is the pseudo-first-order kinetic coefficient, and t is the reaction time.

2.4. Experimental design and process optimization

Response Surface Methodology (RSM) is one of the most widely used methods in the design of experiments for water and wastewater treatment processes (Rahmani et al., 2020). CCD is one of the most widely used RSM technique for modeling the effect of independent variables on system response (Shokoohi et al., 2017). In this study, the effects of four independent variables, i.e., initial solution pH, reaction time, current density, and Na₂SO₄ concentration on system response (MB removal) were modeled by CCD. For this purpose, the effect of four independent variables was investigated at five levels (−α, −1, 0, +1, +α). Table 1 shows the independent variables and their operating ranges. According to Eq. (10), a 5-level-4-factor full CCD contains 30 experiments, of which 16 tests are related to factorial points, 10 tests are indicative of axial points, and 4 tests indicate the repetition in central points. The full CCD scheme with the actual values of the independent variables and the predicted dye removal efficiency can be seen in Table 2. Experimental design and data analysis were performed by Design-Expert 12.0 software (Shokoohi et al., 2019).

$$N = 2^K + 2K + C \quad (10)$$

In this equation, N is the number of experiments designed; K represents the number of independent variables, which is equal to 4 in this study, and C is the number of the experiment repetitions at the central points. 2^K and 2K are the numbers of experiments in the axial and factorial points, respectively. The adequacy of the proposed model for predicting system response and the significance level of linear, interactive, and quadratic effects were determined by the F-value and p-value

Table 1 Four independent variables and their studied levels.

Independent Variables	Symbols	Coded levels					Unit
		−α	−1	0	+1	+α	
pH	A	3	5	7	9	11	–
Reaction Time	B	10	20	30	40	50	min
Current Density	C	2	4	6	8	10	mA/cm ²
Na ₂ SO ₄ concentration	D	20	40	60	80	100	mg/L

Table 2 Full CCD matrix with laboratory and predicted MB removal efficiency.

Run	Variables				MB degradation (%)		Run	Variables				MB degradation (%)	
	A	B	C	D	Experimental	Predicted		A	B	C	D	Experimental	Predicted
1	9	20	8	40	76.6	76.59	16	5	40	4	80	76.2	76.61
2	7	30	6	60	78.5	78.8	17	9	40	8	80	86.1	86.28
3	9	20	4	40	62.7	62.93	18	7	30	6	60	78.6	78.8
4	5	20	4	80	70.5	70.43	19	5	20	8	80	83.6	83.99
5	5	40	8	40	84.4	84.67	20	9	40	4	40	68.9	69.11
6	5	40	4	40	71.5	71.35	21	11	30	6	60	71.3	71.11
7	9	40	4	80	74.4	74.37	22	7	30	6	100	79.4	79.31
8	5	20	4	40	65.1	65.17	23	7	30	6	60	79.2	78.8
9	7	10	6	60	71.3	71.29	24	7	30	6	60	78.5	78.8
10	9	20	4	80	68.2	68.18	25	9	20	8	80	81.2	81.1
11	7	30	6	20	69.7	69.54	26	7	30	10	60	93.4	93.34
12	7	30	2	60	67.3	67.11	27	5	40	8	80	89.5	89.18
13	7	30	6	60	79.2	78.8	28	3	30	6	60	76.3	76.24
14	7	30	6	60	78.8	78.8	29	5	20	8	40	79.7	79.48
15	9	40	8	40	81.6	81.78	30	7	50	6	60	82.9	82.66

obtained by ANOVA analysis of variance. Model quality and accuracy were determined by R² and adj-R² coefficients. Interactive effects of parameters on system response were investigated by 3D and contour response surface plots.

GA and CCD techniques were used to obtain the optimal points of the independent variables and to predict the maximum removal efficiency of MB in the electrochemical degradation system with G/β-PbO₂ anode. In both methods, the basis of the optimization is the final proposed equation of the quadratic model to investigate the effect of input variables on the system response. The GA method is based on Charles Darwin's survival of the fittest theory. The technique is started by generating a random population that has suitable solutions to solve a problem. The best solutions created by a population are used to generate a new population, with the probability that the new population is better than the previous population. To obtain optimal conditions, the above steps continue to improve the population as much as possible (Salari et al., 2019). All optimization steps were performed by the GA technique using MATLAB R2013a software. Finally, the predictions of both GA and CCD methods were compared.

3. Results and discussion:

3.1. Characterization of G/β-PbO₂ anode

SEM images of the graphite plate coated with PbO₂ can be observed at three different magnifications in Fig. 2(a)–(c). As can be seen, PbO₂ is coated on the graphite substrate uniformly and without cracking, mainly in the form of pyramidal clusters and highly compressed structures (Li et al., 2016). The XRD diffractogram of the G/β-PbO₂ anode has shown in Fig. 2(d). The diffraction peaks at 2θ = 25.4°, 32°, 36.2°, 40.4°, 45°, 49.2°, 52.2°, 58.9°, 62.7°, and 67° belong to tetragonal β-PbO₂ which can be indexed with standard JCPDS data card no. 89–2805 (Li et al., 2014). Also, the diffraction peaks observed at 23.6°, 28.5°, 33.1°, 50.7°, 52.2°, and 56.5° belong to the α-PbO₂ phase (JCPDS 72-2440). XRD diffractogram of the G/β-PbO₂ was also analyzed with X'Pert HighScore software. The relevant results are shown in Fig. 2(e). These

results show that the Wt.% of α-PbO₂ phase (Scrutinyite) is 11.7% and the Wt.% of β-PbO₂ phase (Plattnerite) is 88.3%, so the dominant form of PbO₂ on the graphite surface is the β-PbO₂ with the tetragonal structure (Hao et al., 2014). The average crystallite size (D) of β-PbO₂ was calculated by the Debye-Scherrer formula (Eq. (11)) and X'Pert HighScore software (Mandal et al., 2020).

$$D = \frac{K\lambda}{\beta \cos\theta} \quad (11)$$

where K is shape factor (0.9), λ shows the wavelength of the X-ray, β represents full width at half-maximum of the peak in radians, and θ is diffraction angle. In this way, the average crystallite size of β-PbO₂ with both methods was obtained to be about 30.3 nm. Fig. 3 shows the EDX analysis of the G/β-PbO₂ anode. As can be seen, the chemical structure of the film precipitated on the graphite substrate contain 79.1 wt% lead and 20.9 wt% oxygen (Dargahi et al., 2018).

3.2. Modeling of MB degradation and process optimization

To investigate the MB removal in the electrochemical oxidation system using G/β-PbO₂ anode, 30 experiments were presented by CCD experimental design. Table 2 shows the full CCD matrix with the experimental and predicted values of MB removal. Changes in system response to independent parameter changes were first examined by the software. Accordingly, in this study, the MB removal follows a quadratic model. The significance level (p-value) was considered ≤0.05 for the model and all related statistics. Therefore, to achieve a compact model, parameters with p-value >0.05 were excluded from the proposed model. Accordingly, four linear effects (A, B, C, and D), three interactive effects (AC, BC, and CD) and four quadratic effects (A², B², C², and D²) were significant in this study. The results of the data analysis (ANOVA) and Fit Statistics for the reduced quadratic model are shown in Table 3.

The F-value and p-value values of the model are 1674.82 and <0.0001, respectively, which indicates that the reduced model is significant and adequate to predict the system

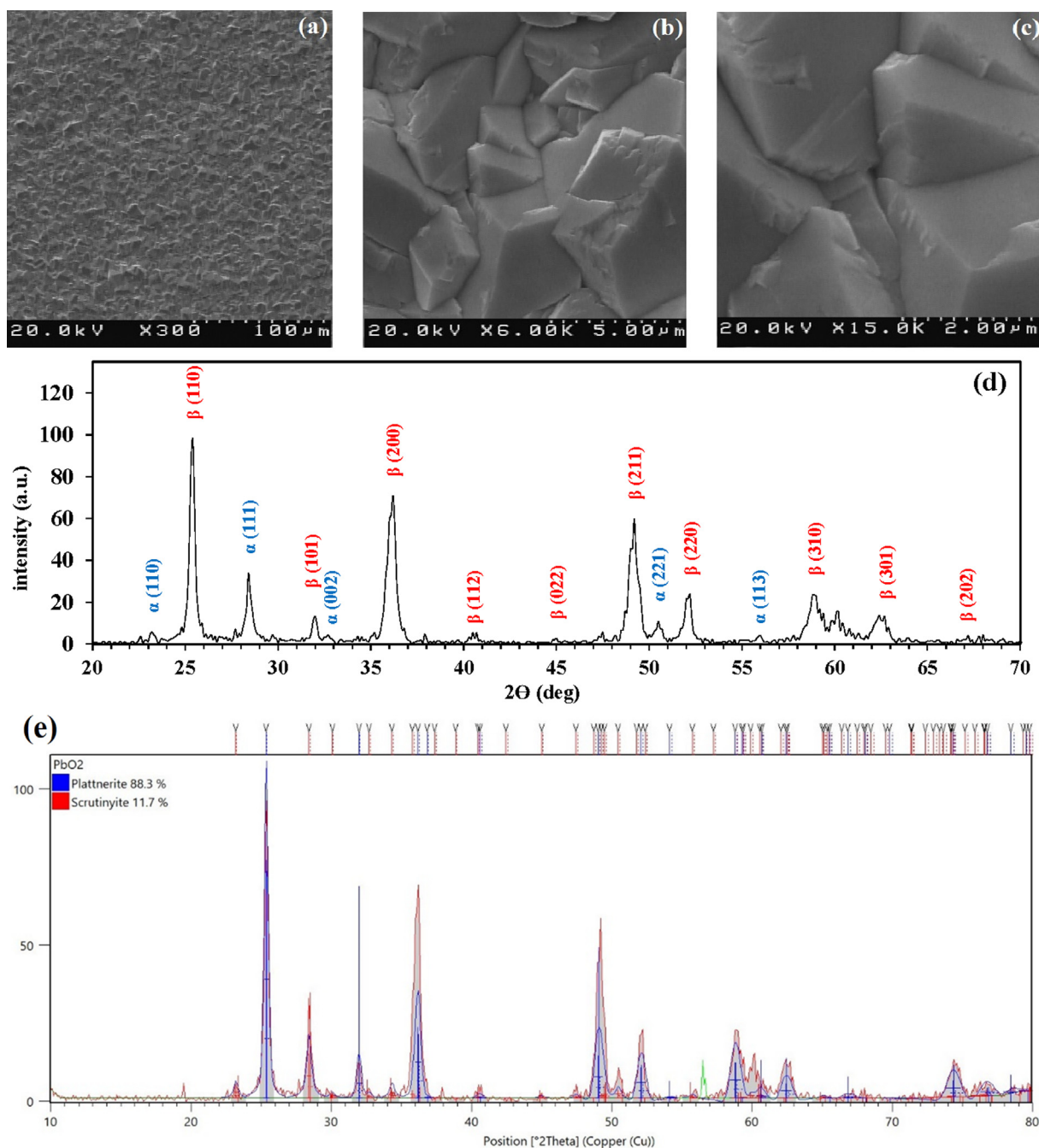


Fig. 2 (a), (b) and (c) SEM images of the G/ β -PbO₂ anode at three different magnifications; (d) XRD diffractogram of the G/ β -PbO₂ anode; (e) The result of X'Pert HighScore software.

response (Salari et al., 2019). The Lack of Fit F-value of 0.6541 implies that the Lack of Fit is not significant compared to the pure error. There is a 75.21% chance that a Lack of Fit F-value this large could occur due to noise. Non-significant lack of fit is good. In other words, the model has well fitted with the available data (Rahmani et al., 2019). The validity of the proposed model was confirmed by high (close to 1) values of the R^2 and adj- R^2 (Ravikumar et al., 2005). In this study, the values of R^2 and adj- R^2 are 0.999 and 0.9984, respectively; on the other hand, if the values of

R^2 and adj- R^2 are close together, it confirms that there is no unnecessary parameter in the proposed model. The Adeq precision parameter statistically represents the signal-to-noise ratio, and values >4 are favorable for the model. In this study, this parameter is 168.96. A model whose variance coefficient (C.V.%) is less than 10% is considered as a reproducible model. In this study, the value of 0.37% indicates a high reproducibility of the modified model. The final equations of the reduced model in terms of actual and coded factors can be observed in Eqs. (12) and (13).

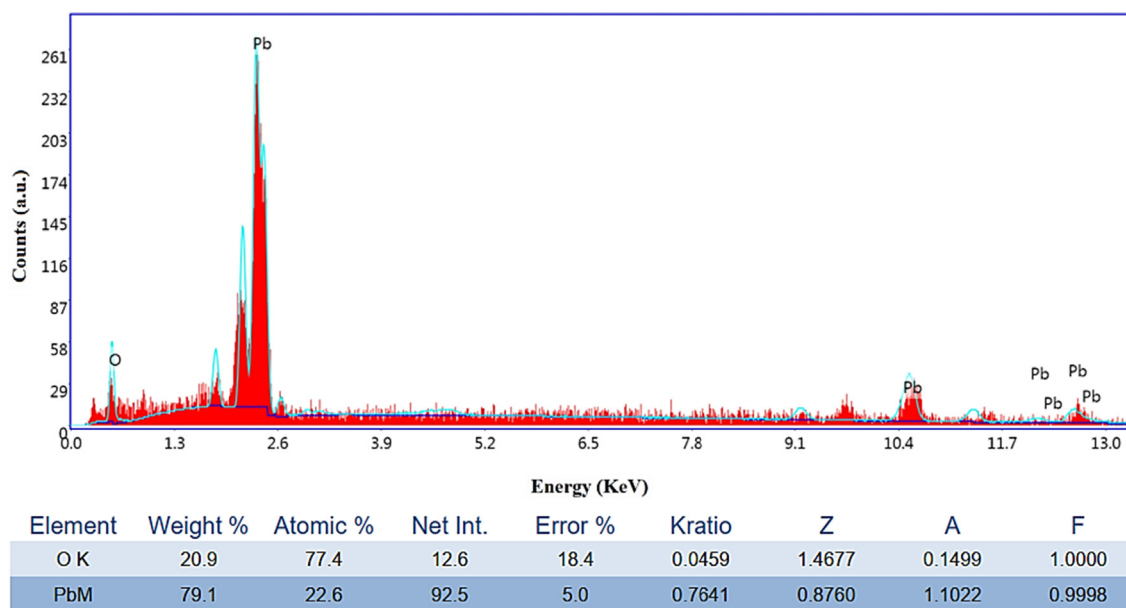


Fig. 3 EDX spectra of the G/β-PbO₂ anode.

$$\begin{aligned}
 \text{MB removal (\%)} = & +15.68385 + 4.08646(\text{pH}) \\
 & + 0.632917(\text{Reaction time}) \\
 & + 3.15104(\text{Current density}) \\
 & + 0.47833(\text{Na}_2\text{SO}_4 \text{ concentration}) \\
 & - 0.040625(\text{pH} \times \text{Current density}) \\
 & - 0.0125(\text{Reaction time} \times \text{Current density}) \\
 & - 0.004688(\text{Current density} \\
 & \times \text{Na}_2\text{SO}_4 \text{ concentration}) - 0.320312(\text{pH}^2) \\
 & - 0.004562(\text{Reaction time}^2) \\
 & + 0.089063(\text{Current density}^2) \\
 & - 0.002734(\text{Na}_2\text{SO}_4 \text{ concentration}^2) \quad (12)
 \end{aligned}$$

$$\begin{aligned}
 \text{MB removal (\%)} = & +78.8 - 2.57A + 5.68B + 13.12C \\
 & + 4.88D - 0.65AC - 1BC \\
 & - 0.75CD - 5.12A^2 - 1.82B^2 \\
 & + 1.43C^2 - 4.37D^2 \quad (13)
 \end{aligned}$$

To further evaluate the adequacy of the proposed model, diagnostic plots were used. The difference between the values obtained from the experimental and predicted values by the model is called residual. The normality of the data can be detected by the normal probability plot of the residuals. Fig. 4(a) shows that all data points are approximately on a central line, that is, the data are normally distributed in the model prediction. Based on Fig. 4(b) and (c), all residuals have randomly scattered within the standard deviation range (± 3.72) and none of the points are out of range. This indicates that there is no need to repeat any of the runs. As shown in Fig. 4(d), the lowest point in the Box-Cox plot (Best lambda = 1) confirms that there is no need to transfer system response (Antonopoulou et al., 2017; Cho and Zoh, 2007).

To predict the maximum removal efficiency of MB in the electrochemical oxidation system with G/β-PbO₂ anode, process optimization was performed by both CCD and GA meth-

ods. In the CCD method, four independent variables were set as input parameters to the model in “in range” mode, and MB removal efficiency was set in “maximize” mode (MB removal = 100%) (Dargahi et al., 2018; Shokoohi et al., 2019). Among the solutions presented, the solution with the highest desirability was selected as the optimal conditions of the oxidation system. The optimal conditions obtained by the CCD method are presented in Fig. 5(a). According to the prediction of the model, the maximum MB removal efficiency, in this case, is 97.68%. An experiment with three repetitions was performed under optimum conditions, in which the MB removal efficiency was 96.2 ± 0.14 . In the GA method, the final equation based on the actual factors (Eq. (12)) was used as the input fitness function, and the input variables were defined in their high and low values ($-\alpha$ and $+\alpha$) (Eqs. (14)–(17)). Population size and type were 250 and double vectors, respectively, and the number of generations was set to 250.

$$3 \leq \text{pH} \leq 11 \quad (14)$$

$$10 \leq \text{Reaction time (min)} \leq 50 \quad (15)$$

$$2 \leq \text{Current density (mA/cm}^2\text{)} \leq 10 \quad (16)$$

$$20 \leq \text{Na}_2\text{SO}_4 \text{ concentration (mg/L)} \leq 100 \quad (17)$$

Fig. 5(b) shows the fitness values versus the number of generations. As can be seen, as the number of generations increases, the average fitness decreases gradually. Finally, after 80 repetitions, the optimum conditions for the removal of MB in the electrochemical oxidation system are presented in Fig. 5(c). Under these conditions, the maximum predicted and experimental removal efficiencies were 98.58 and 97.4 ± 0.17 %, respectively. Fig. 5(d) and (e) display the average distance between individuals and plots of best, worst and mean scores, respectively. By comparing the predicted and experimental removal efficiency values, both optimization methods were found to be able to the prediction of the system response with high accuracy.

Table 3 ANOVA results and Fit Statistics for reduced quadratic model.

ANOVA						
Source	Sum of Squares	df	Mean Square	F-value	p-Value	
Model	1492.61	11	135.69	1674.82	<0.0001	Significant
A	39.53	1	39.53	487.87	<0.0001	
B	193.8	1	193.8	2392.07	<0.0001	
C	1032.28	1	1032.28	12741.31	<0.0001	
D	143.08	1	143.08	1766.04	<0.0001	
AC	0.4225	1	0.4225	5.21	0.0348	
BC	1	1	1	12.34	0.0025	
CD	0.5625	1	0.5625	6.94	0.0168	
A ²	45.03	1	45.03	555.76	<0.0001	
B ²	5.71	1	5.71	70.47	<0.0001	
C ²	3.48	1	3.48	42.97	<0.0001	
D ²	32.81	1	32.81	405	<0.0001	
Residual	1.46	18	0.081			
Lack of Fit	0.9183	13	0.0706	0.6541	0.7521	Not significant
Pure Error	0.54	5	0.108			
Cor Total	1494.07	29				

Fit Statistics results: $R^2 = 0.999$, Adjusted $R^2 = 0.9984$, Adeq Precision = 168.9622 and C.V (%) = 0.3705.

To determine the effect of each parameter on the system response (MB dye removal efficiency), the Pareto effect for each parameter (P_i) was calculated by Eq. (18).

$$P_i(\%) = \left(\frac{\beta_i^2}{\sum \beta_i^2} \right) \times 100 \quad (18)$$

In this equation, β_i is the regression coefficient of each parameter in the final model equation in terms of coded factors, which were represented in Eq. (13). As shown in Fig. 5 (f), the highest effect, among the four independent variables, were current density (+59.88%), reaction time (+11.22%), Na_2SO_4 concentration (+8.28%) and solution pH (−2.30%), respectively. Among the interactive effects, the highest percentage of the effect belongs to the interaction between reaction time and current density (BC). Among the quadratic effects, the most significant was the solution pH (A^2).

3.3. Effect of independent variables on MB removal efficiency

3.3.1. The effect of solution pH

Interactive effect between initial solution pH and reaction time has shown in Fig. 6(a) and (b). At an initial MB concentration of 60 mg/L, a current density of 10 mA/cm² and Na_2SO_4 concentration of 78.8 mg/L, the MB removal efficiency increases with decreasing pH and increasing reaction time. As shown in Fig. 6(b), the highest MB removal efficiency (97.67%) was predicted at the pH of 5.75 and the reaction time of 50 min. In contrast, the lowest removal efficiency of 79.67% was observed at the pH of 11 and the reaction time of 10 min. One of the most important parameters influencing the development of electrochemical processes is the initial solution pH; as mentioned earlier, PbO_2 anode is classified in the group of non-active anodes with high oxygen evolution potential. The main mechanism of degradation of organic pollutants in this type of the anodes is the formation of HO^\cdot , the HO^\cdot produced on the surface of PbO_2 anodes have a short life time, and then, it is not participating for oxidizing in the solution. Actually, it

acts in the Nernst layer, close to the anode (reaction cage) (Abu Ghalwa et al., 2016). On the other hand, the HO^\cdot oxidation potential is strongly dependent on the pH of the aqueous solution, and with increasing reaction solution pH, its oxidation potential is dramatically reduced from 2.4 to 2.7 V under acidic conditions to approximately 1–1.29 V under alkaline conditions (Neta et al., 1988).

In the anodic oxidation system, there is always a competition for the reaction of oxygen evolution and oxidative degradation of organic matter on the anode. Increasing the pH of the solution reduces the oxygen evolution potential and, consequently, elevates the rate of oxygen evolution at the anode surface; this subdues the rate of diffusion of organic pollutants to the anode, which ultimately reduces the oxidation rate of the organic matter at the anode surface (Zhao et al., 2019). Conversely, under acidic conditions, as the oxygen evolution reaction subsided, the electrochemical conditions for the degradation of organic pollutants at the anode surface are strengthened (Neto and De Andrade, 2009). In addition, under alkaline conditions, due to the high consumption rate of supporting electrolyte, the conductivity of the solution falls due to the lack of sufficient electrolyte, and thus, the degradation efficiency of organic pollutants further declines (Dai et al., 2013). In a study performed by Fernanda et al., for degradation of dimethyl phthalate ester using fluoride-doped Ti/ β - PbO_2 anode, the kinetics of the contaminant removal at pH = 3 was higher than pH values of 7 and 10 (Souza et al., 2014). In a study conducted by Samet for the electrochemical degradation of 4-chloroguaiacol with Nb/ PbO_2 anodes, an increase in pH in the range of 2–6 reduced the kinetics of contaminant removal (Samet et al., 2006). In addition, the highest electrochemical degradation efficiency of Methyl Orange using Nb/ PbO_2 anode was achieved at an initial pH of 6 (Yang et al., 2016).

3.3.2. The effect of current density

The influence of current density and initial solution pH on MB dye removal efficiency were shown in Fig. 6(c) and (d). It is

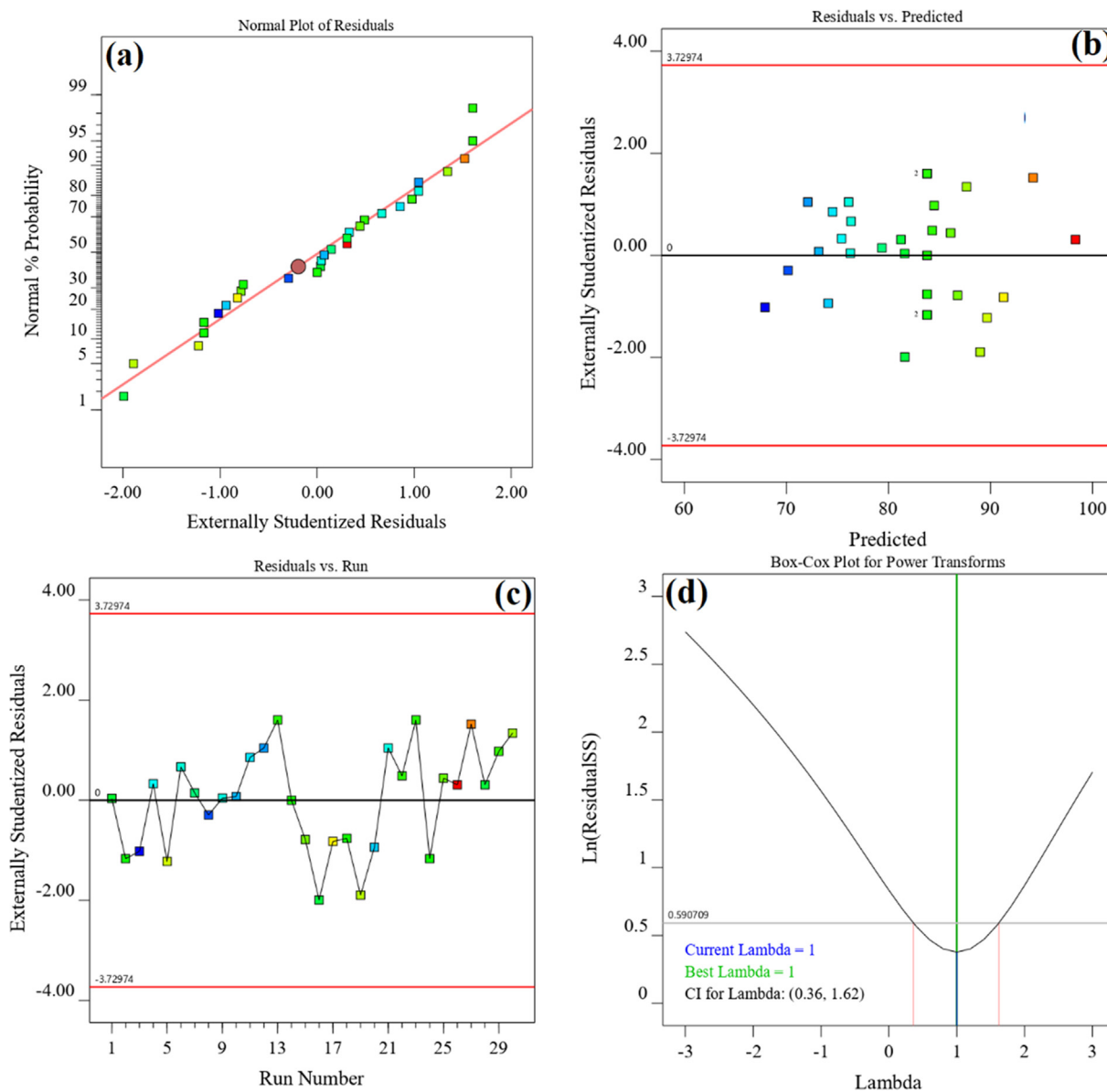


Fig. 4 The diagnostic plots for validation of obtained model: (a) normal plot of residuals, (b) residuals versus predicted, (c) residuals versus run order and (d) Box-Cox Plot.

pretty obvious that increasing the current density from 2 to 10 mA/cm² at the pH of 11 is led to rise the MB dye removal efficiency from 66.7% to about 88.64%. Also, Fig. 6(c) shows that at pH of 5.7 and current density of 10 mA/cm², MB removal efficiency is about 97.6%. Among the variables affecting the electrochemical oxidation process, the current density has been found as one of the most vital variables that can control the reaction rate of electrochemical degradation (Ansari and Nematollahi, 2018; Nakamura et al., 2019). In general, the increase in the performance of electrochemical oxidation systems by increasing the current density at a constant time is due to the increase in the rate of water oxidation at the anode surface and the enhancement in the production rate of HO[•] (Dai et al., 2016; Wang et al., 2015). On the other hand, applying the greater current density to the electrochemical cell prevents the inactivation of the electrochemically active sites

on the anode surface by the intermediates produced during the electrolysis process. However, a much higher current density may further enhance the immediate and adverse reactions of oxygen evolution at the anode surface, which competes with the oxidation of organic matter at the anode surface and, ultimately, reduces the efficiency of organic pollutant removal in electrochemical degradation systems (Ansari and Nematollahi, 2018; Wang et al., 2016; Yao et al., 2019a). Therefore, in this study, MB dye degradation was favorable at low current densities from 2 to 10 mA/cm². Qiang Zhao et al., used lead dioxide anodes for electrochemical treatment of coal tar wastewater, and reported that the COD removal efficiency of wastewater was increased from 75% to about 93% by increasing the current density from 2 to 5 A/dm² (Zhao et al., 2019). Also, in a study conducted by Duan et al., for the electrochemical degradation of phenol by lead

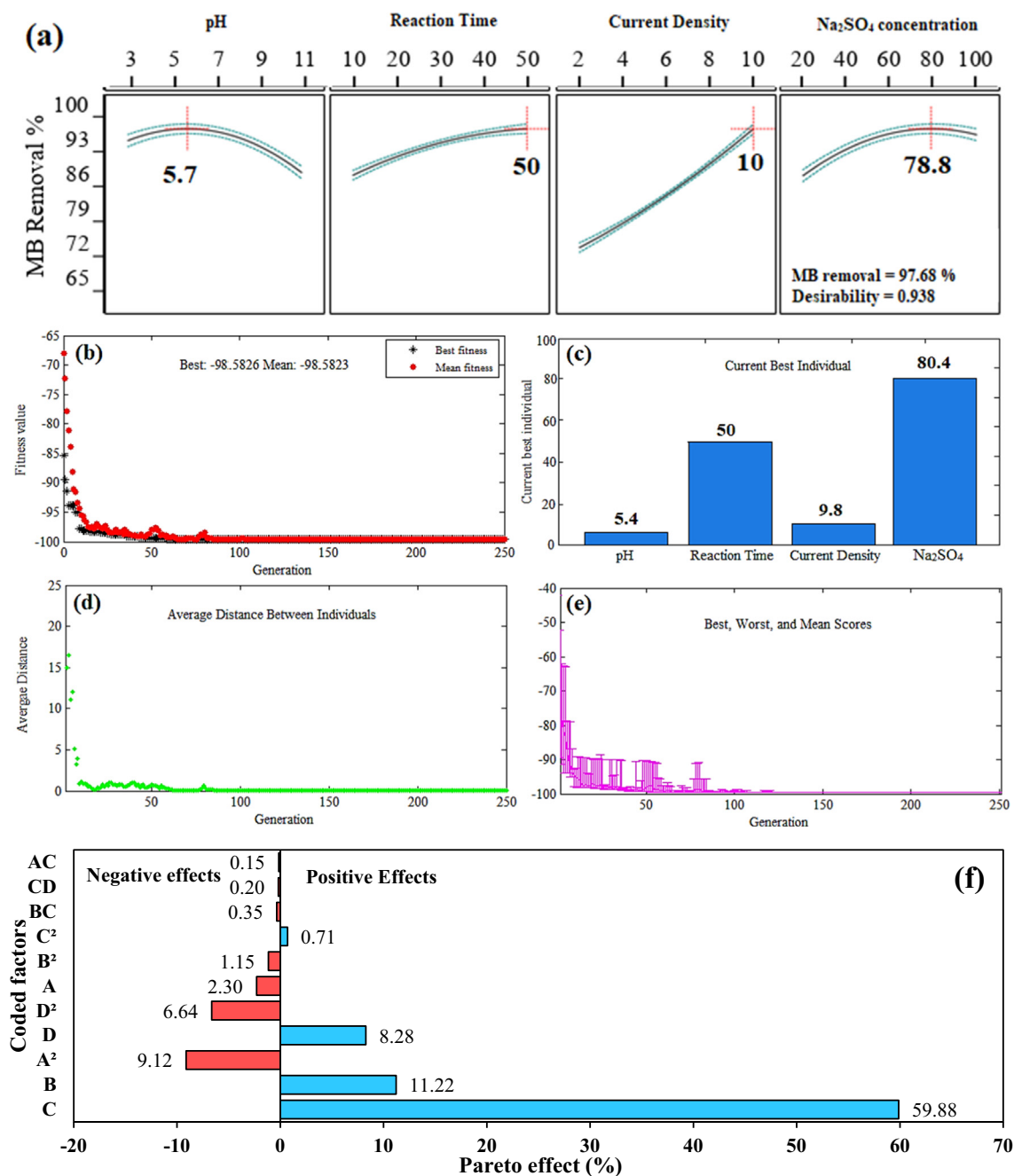


Fig. 5 (a) The optimal points obtained by CCD method; (b), (c), (d) and (e) The optimal points obtained by GA method; (f) The Pareto effect of each term on MB removal.

dioxide anode, the phenol removal efficiency was increased from about 19% to 79% by increasing the current density in the range of 10–50 mA/cm² (Duan et al., 2013).

3.3.3. The effect of Na₂SO₄ concentration

The use of a supporting electrolyte to improve the electrical current transfer in the solution mass is an indispensable factor in the electrochemical oxidation processes of organic compounds; in various studies, NaCl (Aquino et al., 2014) and Na₂SO₄ (Yang et al., 2016) have been employed for this purpose. In the present study, the effect of different concentrations of Na₂SO₄ electrolyte on MB removal efficiency was

investigated in the range of 20–100 mg/L. As shown in Fig. 7(a) and (b), it is observed that, at a constant current density of 10 mA/cm², the dye removal efficiency was improved from 84% to about 97.7% by increasing Na₂SO₄ concentration from 20 mg/L to 78 mg/L. However, a further increase in Na₂SO₄ electrolyte concentration from 80 to 100 mg/L slightly diminished the removal efficiency of MB. Therefore, the optimum Na₂SO₄ electrolyte concentration was 78.8 mg/L in the present study. Increasing the electrolyte concentration of Na₂SO₄ improves the conductivity of the solution by facilitating electron transfer and increasing the rate of production of HO[•] at the anode surface. On the other hand, based on

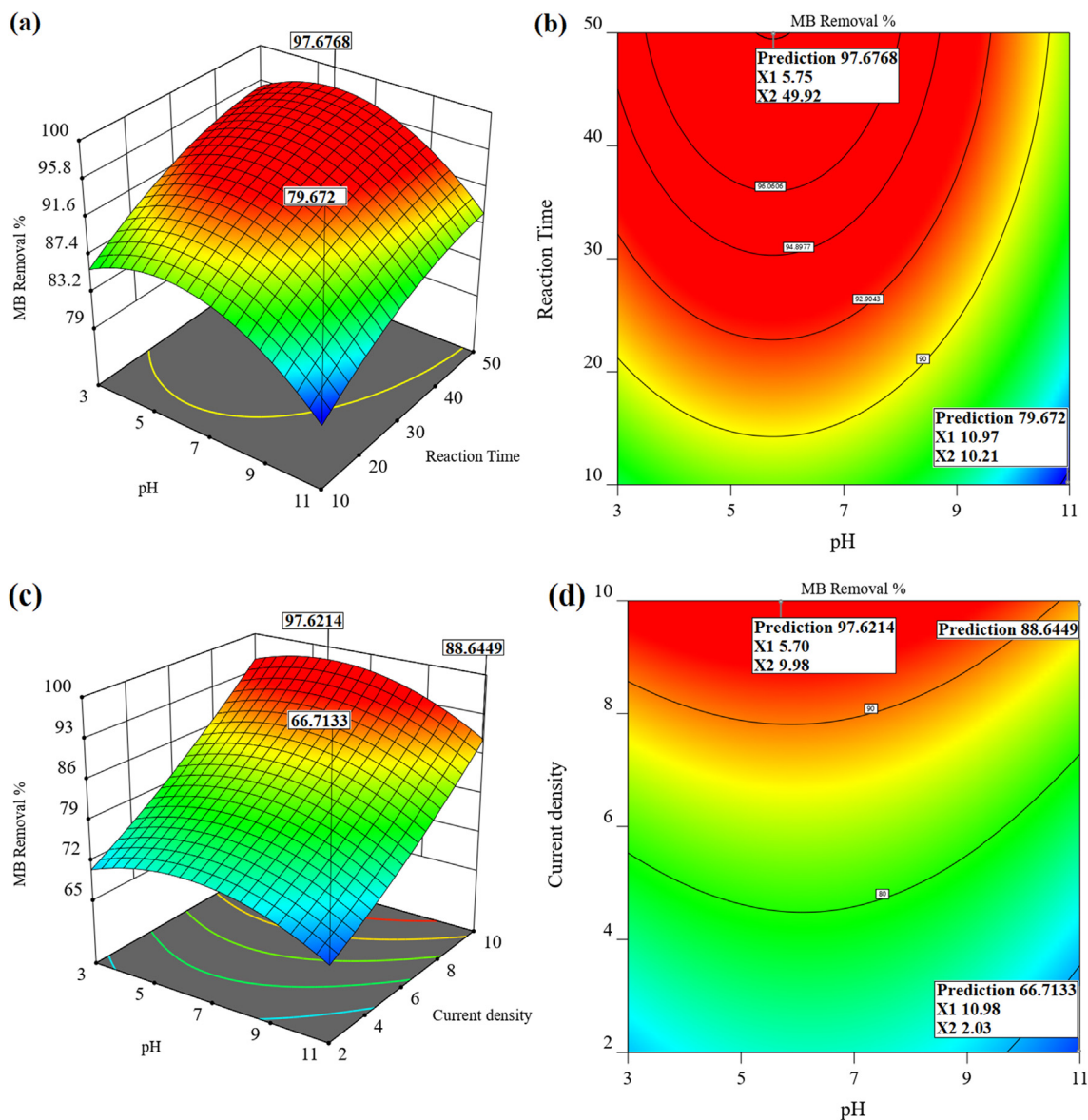


Fig. 6 (a) 3D and (b) contour response surface plots showing the interaction of pH and reaction time (MB = 60 mg/L, Current density = 10 mA/cm², Na₂SO₄ = 78.8 mg/L); (c) 3D and (d) contour response surface plots showing the interaction of pH and current density (MB = 60 mg/L, Reaction time = 50 min, Na₂SO₄ = 78.8 mg/L).

the reports, BDD and PbO₂ anodes are capable of producing radicals from anions in solution. Eqs. (19) and (20) show the formation of sulfate and chlorine radicals (Sirés et al., 2014):



However, at high concentrations of Na₂SO₄, excess sulfate ions (SO₄²⁻) migrate to the anode and accumulate at its surface. Occupying the active sites on the surface of the anode with SO₄²⁻ ions results in inactivation of the electrocatalytic property of the anode, and as a result, it is led to reducing the organic pollutant removal efficiency (Dai et al., 2016). In a study conducted by Yao et al., for electrochemical removal of thiamethoxam using PbO₂-CeO₂ anode, an increase in Na₂SO₄ electrolyte concentration decreased the removal

efficiency of the contaminant (Yao et al., 2018). In addition, Yang studied the removal of Methyl Orange using Nb/PbO₂ anode and determined the optimum Na₂SO₄ electrolyte concentration as 0.08 mol/L (Yang et al., 2016).

3.4. Comparison performance of G/β-PbO₂ and graphite anode and degradation kinetic

To determine the effect of β-PbO₂ electrocatalyst on MB dye removal, the performance of graphite and G/β-PbO₂ anodes were compared for electrochemical MB removal at three concentrations of 60, 120 and 180 mg/L under optimum conditions (pH = 5.75, Current density = 10 mA/cm², Na₂SO₄ = 78.8 mg/L). The results of this comparison are shown in Fig. 8. The comparison of Fig. 8(a) and (b) indicates that the MB removal efficiency by the G/β-PbO₂ anode is

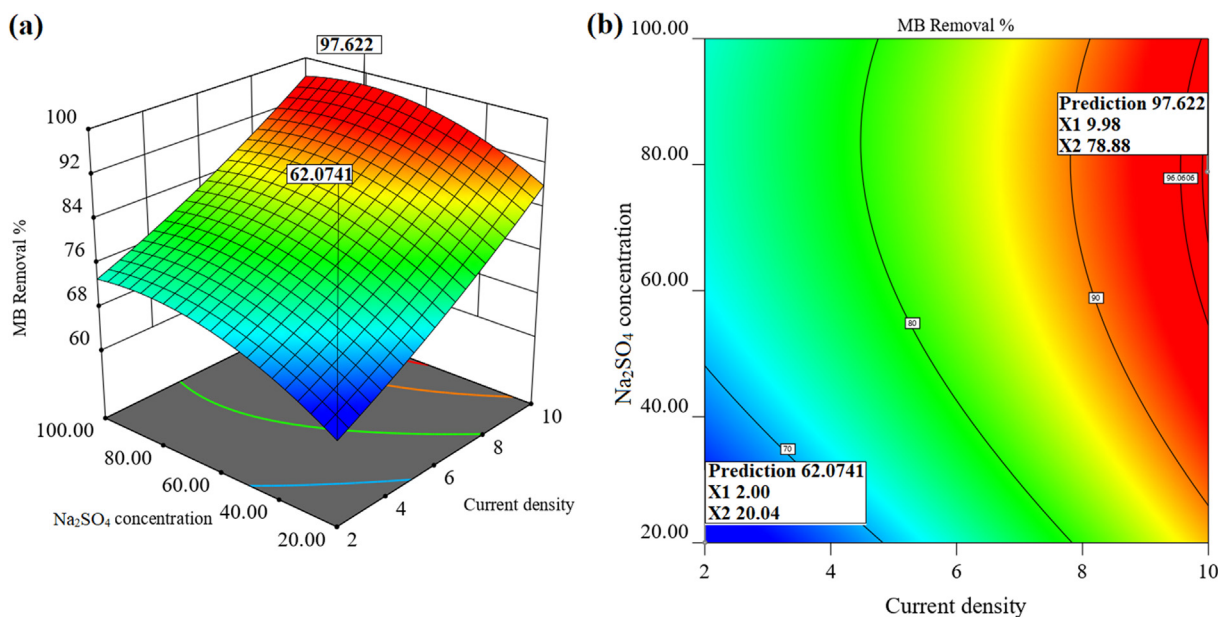


Fig. 7 (a) 3D and (b) contour response surface plot showing the interaction effect of Na₂SO₄ concentration and current density (MB = 60 mg/L, Reaction time = 50 min, pH = 5.75).

significantly higher than that of graphite anode. So that at MB concentration of 60 mg/L, the removal efficiencies for graphite and G/ β -PbO₂ anodes at the reaction time of 10 min were 25% and 87%, respectively. At the same conditions, the removal efficiencies for graphite and G/ β -PbO₂ anodes at the end of 60 min were 68.3% and 96.4%, respectively. Graphite anode is classified in the group of active anodes with low oxygen evolution potential based on nature, hence the dominant mechanism for oxidation and degradation of the contaminant by this anode is direct electron transfer from the organic contaminant to the anode surface (Abdalkhman et al., 2019). The graphs related to the kinetics of MB degradation in the electrochemical system with G/ β -PbO₂ and graphite anodes are shown in Fig. 8(c) and (d), respectively. Fig. 8(e) shows the kinetic coefficients of electrochemical removal of MB dye under optimum operational conditions. As can be seen, the electrochemical removal of MB dye by graphite and G/ β -PbO₂ anode well corresponds to the pseudo-first-order kinetic model ($R^2 > 0.9$). Additionally, the kinetic coefficients (k_{obs}) of electrochemical removal of MB dye by G/ β -PbO₂ anode was decreased by about 1.42 times with increasing initial dye concentration from 60 to 180 mg/L. In addition, at a constant MB dye concentration of 60 mg/L, the kinetic coefficient of electrochemical dye removal by the G/ β -PbO₂ anode is about 2.62 times higher than that of graphite anode. Samarghandi et al., have used graphite anode to remove 2,4-D herbicides; based on their reports, increasing the current density in the range of 1 to 5 mA/cm² has resulted in an increase in the oxidation system efficiency, so that 2,4-D removal efficiency at initial concentrations of 50 and 100 mg/L under the conditions including the current density of 5 mA/cm², pH of 3 and 80 min were 98% and 69%, respectively (Samarghandi et al., 2019). Also, in Fig. 8(a) and (b), it is reasonably clear that for both anodes, an increase in the initial concentration of MB dye from 60 to 180 mg/L reduces the removal efficiency. For the

G/ β -PbO₂ anode, at the reaction time of 60 min, MB dye removal efficiency at initial dye concentrations of 60 and 180 mg/L was 96.4 and 85%, respectively. Under the same conditions, removal efficiencies using graphite anode was 68.3% and 46%, respectively. At low concentrations of organic pollutant, the kinetics of electrochemical degradation reactions are faster than the rate of contaminant mass transfer to the anode surface; thus, the efficiency of removal of organic pollutants is increased and in other words, the performance of the electrochemical removal reaction is improved. However, under constant operational conditions, by increasing the initial MB concentration, more contaminants get closer to the anode surface, while the HO[•] is not sufficient to degrade them, and thus, removal efficiency is reduced. On the other hand, by increasing the initial concentration of the pollutant, more intermediates are produced which compete with the parent molecules of the pollutant through reaction with the HO[•]. Hence, the ratio of radical to pollutant will further decrease (Song et al., 2010). On the other hand, some intermediates produced during oxidation may be adsorbed onto the anode surface, which may lead to inactivate the electrocatalyst sites (Lin et al., 2013; Wang et al., 2010).

3.5. Mineralization, and degradation mechanism of MB

TOC analysis was used to confirm MB mineralization in the electrochemical oxidation system with G/ β -PbO₂ anode. Fig. 9(a) shows the TOC reduction rate in optimal conditions as a function of time in the range of 0 to 60 min. According to the results, 60 min is required for the complete mineralization of MB. The cyclic voltammograms of MB during the anodic oxidation with G/ β -PbO₂ anode are shown in Fig. 9(b). As can be seen, within 0 to 60 min, the oxidation and reduction peaks of MB have been steadily decreased. These results confirm the MB degradation during the process.

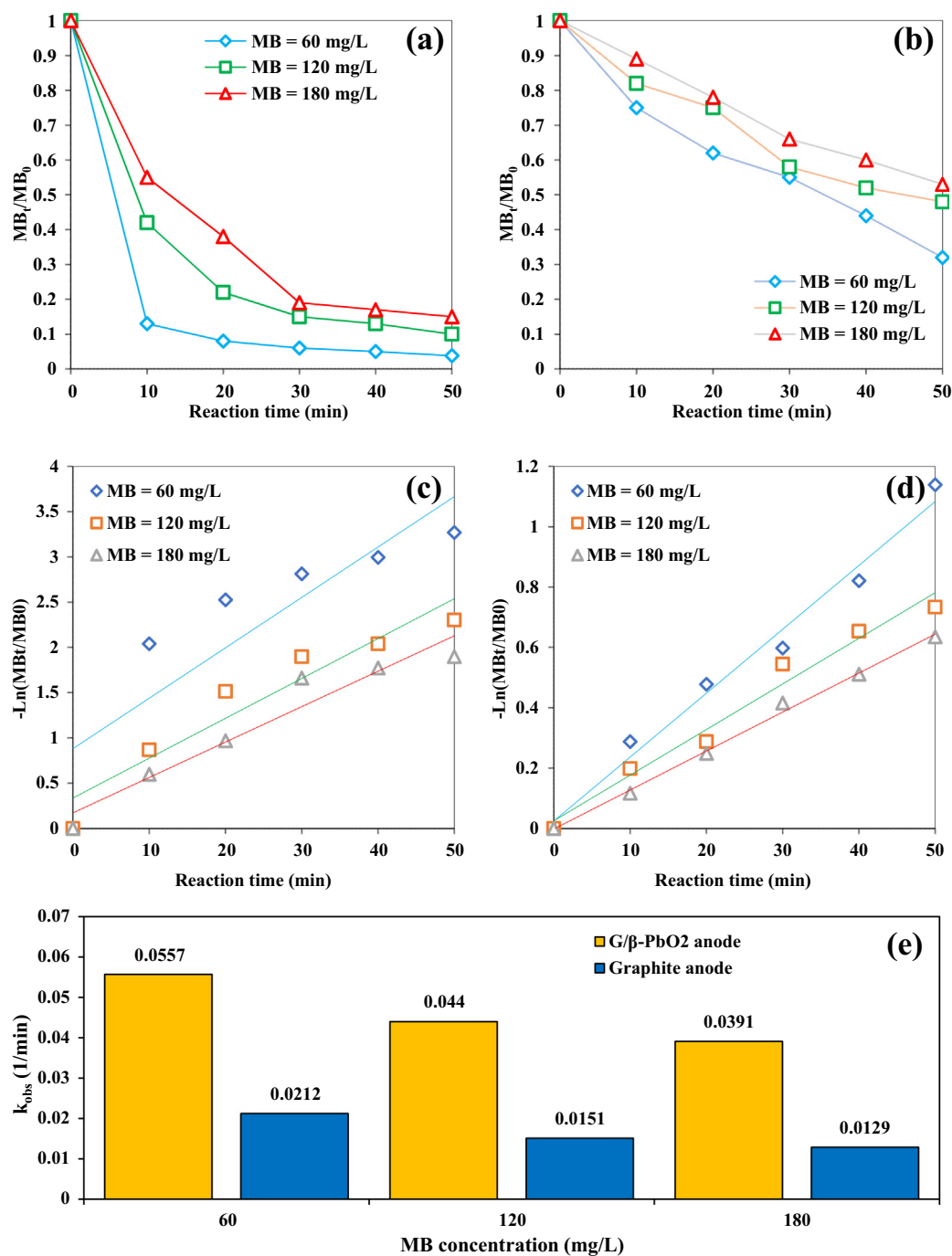


Fig. 8 Effect of different concentrations of MB on removal efficiency and reaction kinetics in the electrochemical oxidation system using (a) and (c) G/β-PbO₂ anode and (b) and (d) graphite anode. (e) Kinetic coefficients of electrochemical removal of MB dye in electrochemical oxidation system using G/β-PbO₂ and graphite anodes.

Intermediates produced by electrochemical degradation of MB were identified by LC-MC analysis. Table 4 shows the chemical structures and names of the identified intermediate compounds. According to the results, the most abundant intermediates produced were compounds with $m/z < 150$, which confirms the degradation of MB ($m/z = 319$). Meanwhile, cyclohexane, cyclohexa-2,5-dien-1-ylum, and N-(sec-butyl) aniline was identified as the most abundant compounds. Finally, a degradation pathway was proposed for the degrada-

tion of MB in the electrochemical oxidation system using G/β-PbO₂ anode. Fig. 10 demonstrates that ROS (HO[•]) can cause the hydroxylation process by adding OH to the MB compound. This effect can be observed in the formation of 7-(methyl-14-azanylyl)-514-phenothiazine-3,5,5 (10H)-triol ($m/z = 279$), 7-(methyl-14-azanylyl)-5,10-dihydro-514-pheno thiazine-3,5-diol ($m/z = 263$) and 4-((4-(methyl-14-azanylyl)phenyl)amino) phenol ($m/z = 215$). The other role of active oxygen groups is to oxidize and hydrolyze the compounds in

the presence of water. This effect is proved by the formation of 4-(phenyl-14-azaneylidene) cyclohexa-2,5-dien-1-imine ($m/z = 181$) and cyclohexa-2,5-dien-1-ylidene(phenyl)-14-azane ($m/z = 170$). The HO \cdot radical is able to cleavage the rings in the structure of the intermediates through ring-opening reactions and eventually produce the pent-1-ene compound. Finally, CO $_2$ and H $_2$ O can be considered as final products of MB degradation.

3.6. Reusability of G/ β -PbO $_2$ anode

High electrocatalytic activity along with high reusability are the main characteristics of an ideal anode for use in electrochemical oxidation processes (Li et al., 2017). In this study, the reusability of the prepared G/ β -PbO $_2$ anode was investigated for fifteen consecutive electrochemical oxidation experiments under optimal conditions. As shown in Fig. 11(a), after fifteen reuses of G/ β -PbO $_2$ anode, the removal efficiency of MB was reduced by only about 2%. These findings exhibit the high reusability of G/ β -PbO $_2$ anode (Xu et al., 2019). The concentration of lead released from the G/ β -PbO $_2$ anode at the end of the 15th oxidation cycle was probed by cyclic voltammetry analysis. The relevant results are presented in Fig. 11(b). If lead enters the treated sample, its peak should be seen in the cyclic voltammetry. As can be seen, no peak is observed on the voltammogram "a" which is related to the treated solution. However, after adding 0.5 mg/L of Pb(NO $_3$) $_2$ to the treated solution, the oxidation peak of lead was observed at -0.5 V vs Ag/AgCl (voltammogram "b").

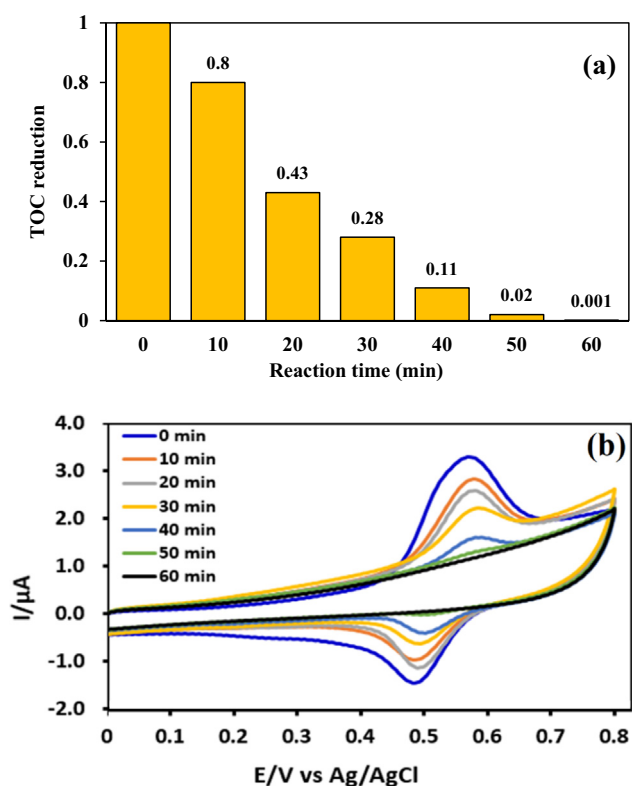
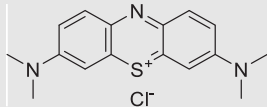
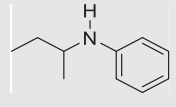
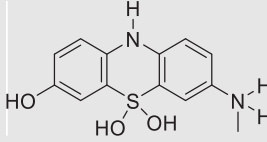
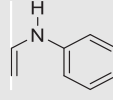
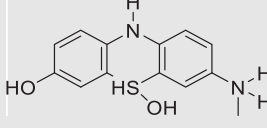
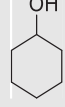
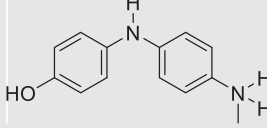
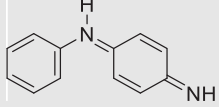
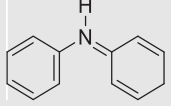


Fig. 9 (a) TOC reduction rate in electrochemical oxidation system with G/ β -PbO $_2$ anode; (b) cyclic voltammograms of MB during electrochemical oxidation process with the G/ β -PbO $_2$ anode.

Table 4 Intermediate compounds identified during the MB electro degradation.

Structure and chemical name	m/z	Structure and chemical name	m/z
 Methylene Blue	319	 N-(sec-butyl) aniline	149
 7-(Methyl-14-azaneyl)-5,14-phenothiazine-3,5,5(10H)-triol	279	 N-vinyl aniline	119
 7-(Methyl-14-azaneyl)-5,10-dihydro-5,14-phenothiazine-3,5-diol	263	 Cyclohexanol	101
 4-((4-(Methyl-14-azaneyl) phenyl) amino) phenol	215	 Cyclohexane	85
 4-(Phenyl-14-azaneylidene) cyclohexa-2,5-dien-1-imine	181	 Cyclohexa-2,5-dien-1-ylum	79
 Cyclohexa-2,5-dien-1-ylidene (phenyl)-14-azane	170	 Pent-1-ene	71

By comparing the two voltammograms, it is concluded that no lead ions leak from the anode surface to the sample solution. These results confirm the stability of the prepared anode. However, ICP analysis showed that the concentration of lead leaked into the solution is 0.0015 mg/L.

3.7. Textile wastewater treatment

After investigating and optimizing the influence of important operational parameters on the efficiency of the MB electrochemical oxidation process using G/ β -PbO $_2$ anode, the performance of the optimized process was evaluated for the

Table 5 The main characteristics of the textile wastewater samples before and after the treatment.

Parameter	Before treatment	After treatment	
		Method I: With pH adjustment	Method II: Without adjusting the pH
pH	8.2	4.9	6.9
BOD (mg/L)	295	195	215
COD (mg/L)	1075	405	570
$\frac{BOD}{COD}$	0.27	0.48	0.37

treatment of real wastewater of local textile industry (Nakh rang Co.). Required samples were taken from the wastewater stream at the outlet of the industrial plant and before entering the treatment plant, and the pH was immediately measured. The samples were treated by two different methods.

In method I, the pH of the samples was adjusted to the optimum value prior to the treatment process (pH = 5.7), however, in method II, the pH of the samples was the same value recorded in the treatment plant (pH = 8.2). As shown in Table 5, the final pH of the samples was reduced after treatment by both methods. In electrochemical oxidation systems, a decrease in pH during the electrolysis process has been reported. In a study, Xu evaluated the degradation of perfluorooctanoic acid by Zr-PbO₂ anode and reported that the final pH of the studied samples was decreased from about 4.8 to about 3 (Xu et al., 2017). Also, according to Wang et al., the final pH of the samples in the electrochemical degradation sys-

tem of ciprofloxacin by the SnO₂-Sb/Ti anode was always associated with a decrease; in addition, the decrease in pH values was higher for the samples with higher initial pH. An appropriate indicator for determining the biodegradability of wastewater is its BOD/COD ratio. Accordingly, wastewater with BOD/COD ≥ 0.4 is considered to be biodegradable (Shabanloo et al., 2020). As can be seen, the biodegradability of the textile wastewater sample after treatment by two methods I and II reached about 0.48 and 0.37, respectively, which symbolizes an increase in its biodegradability. In addition, as can be seen, the removal efficiencies of BOD and COD by treatment method I were about 33.4% and 62.3% and were about 27% and 46% by treatment method II, respectively. The higher COD removal efficiency, compared to BOD removal efficiency, specifies the presence of non-biodegradable organic compounds in the samples studied.

4. Conclusion

This study was performed to optimize the removal of MB dye in the electrochemical oxidation system using G/ β -PbO₂ anodes. SEM and XRD analyses showed that the lead oxide film was uniformly coated on the graphite substrate in the form of the pyramid clusters and highly compact structure in the β -PbO₂ phase. In addition, EDX analysis confirmed a high percentage of lead in the coating. The results of ANOVA (p-value < 0.0001) and Fit Statistics ($R^2 = 0.999$) showed that the reduced quadratic polynomial model is able to accurately predict MB removal efficiency in the electrochemical degradation system by G/ β -PbO₂ anode. Among the four independent variables, the greatest effect on system response was related to current density, reaction time, Na₂SO₄ concentration, and solution pH, respectively. The optimum conditions for

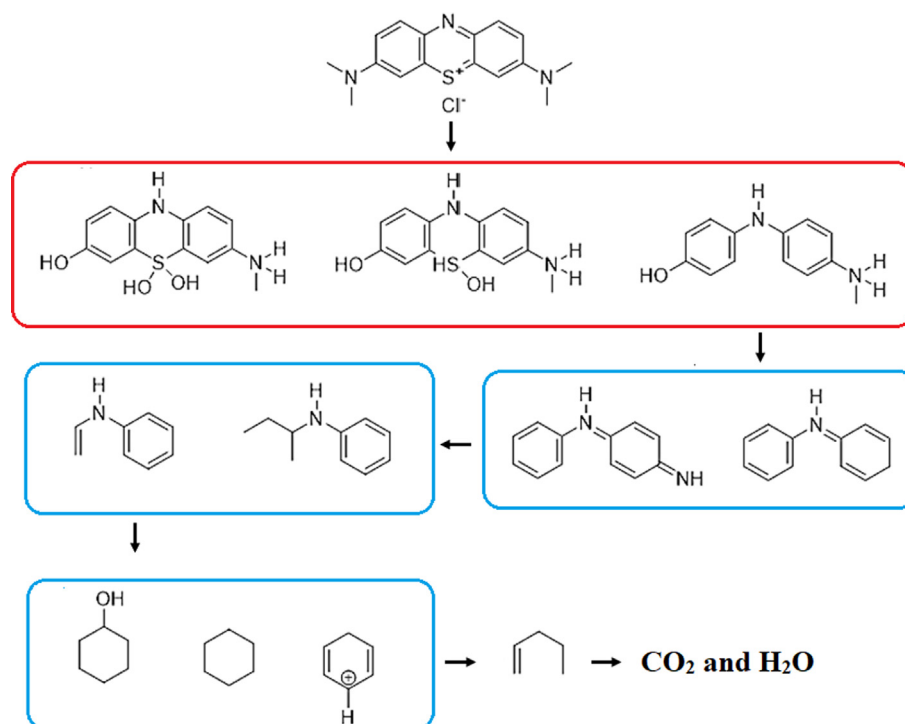


Fig. 10 Proposed pathway for degradation of MB in electrochemical oxidation process with the G/ β -PbO₂ anode.

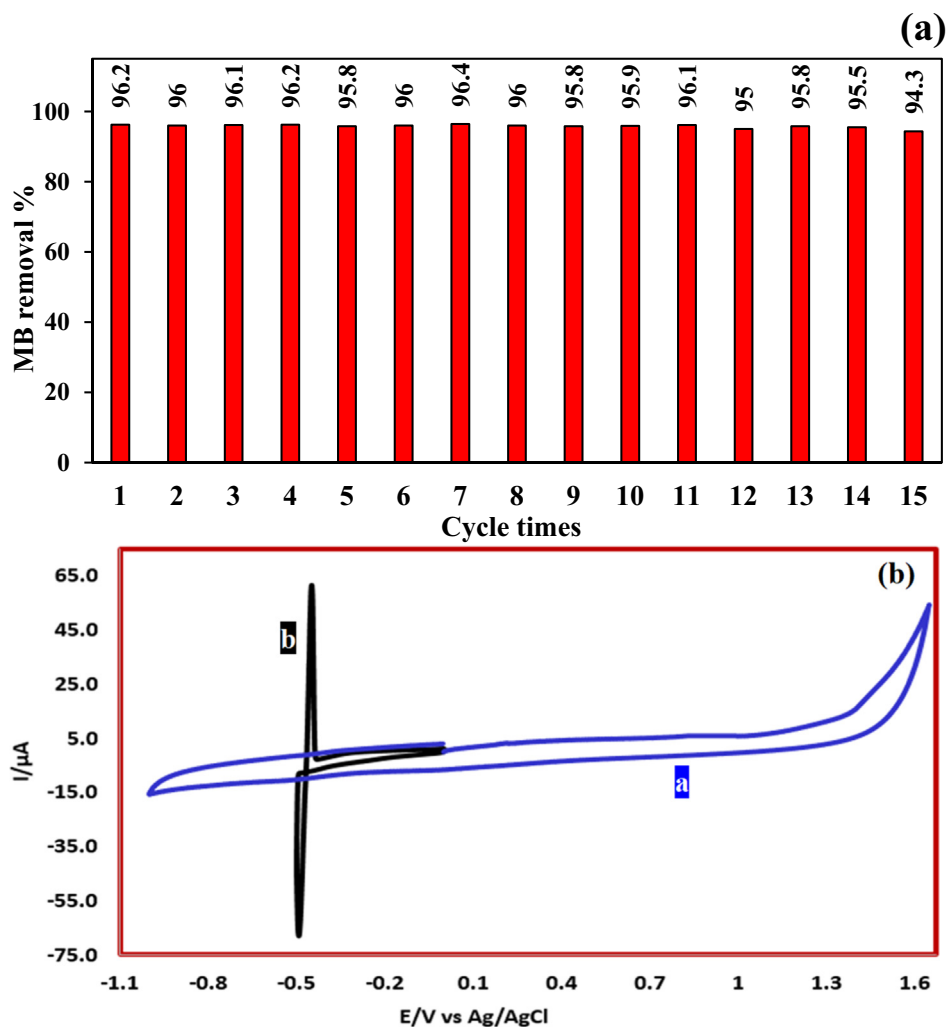


Fig. 11 (a) Reusability of G/ β -PbO₂ anode for electrochemical degradation of MB; (b) Cyclic voltammetry of treated sample and treated sample containing 0.5 mg/L of Pb(NO₃)₂ at glassy carbon electrode (Scan rate = 100 mV/s, Temperature: 25 ± 1 °C).

removal of 96.4% MB dye with an initial concentration of 60 mg/L were obtained at the current density of 10 mA/cm², the reaction time of 50 min and Na₂SO₄ of 78.8 mg /L. The electrochemical removal of MB dye well corresponded to the pseudo-first-order kinetic model. At optimum operational conditions, the kinetic coefficient of electrochemical dye removal by the G/ β -PbO₂ anode was about 2.62 times higher than that of graphite anode. The most abundant intermediates produced by the degradation of MB were compounds (cyclohexane, cyclohexa-2,5-dien-1-ylum and N-(sec-butyl) aniline) with $m/z < 150$. Complete mineralization of MB in the range of 0 to 60 min was confirmed by TOC analysis. Finally, the optimized electrochemical degradation process with G/ β -PbO₂ anode could effectively increase the BOD/COD ratio of the real sample of textile wastewater.

Funding

This work was supported by the Hamadan University of Medical Sciences [grant number: 9710186168].

References

- Abdalkhman, A.S., Ganiyu, S.O., El-Din, M.G., 2019. Degradation kinetics and structure-reactivity relation of naphthenic acids during anodic oxidation on graphite electrodes. *Chem. Eng. J.* 370, 997–1007.
- Abu Ghalwa, N., Hamada, M., Abu Shawish, H.M., Shubair, O., 2016. Electrochemical degradation of linuron in aqueous solution using Pb/PbO₂ and C/PbO₂ electrodes. *Arab. J. Chem.* 9, S821–S828. <https://doi.org/10.1016/j.arabjc.2011.08.006>.
- Alver, E., Metin, A.Ü., Brouers, F., 2020. Methylene blue adsorption on magnetic alginate/rice husk bio-composite. *Int. J. Biol. Macromol.*
- Anglada, A., Urtiaga, A., Ortiz, I., 2009. Contributions of electrochemical oxidation to waste-water treatment: fundamentals and review of applications. *J. Chem. Technol. Biotechnol.* 84, 1747–1755.
- Ansari, A., Nematollahi, D., 2018. A comprehensive study on the electrocatalytic degradation, electrochemical behavior and degradation mechanism of malachite green using electrodeposited nanostructured β -PbO₂ electrodes. *Water Res.* 144, 462–473. <https://doi.org/10.1016/j.watres.2018.07.056>.

- Antonopoulou, M., Chondrodimitou, I., Bairamis, F., Giannakas, A., Konstantinou, I., 2017. Photocatalytic reduction of Cr (VI) by char/TiO₂ composite photocatalyst: optimization and modeling using the response surface methodology (RSM). *Environ. Sci. Pollut. Res.* 24, 1063–1072.
- Aquino, J.M., Rocha-Filho, R.C., Ruotolo, L.A.M., Bocchi, N., Biaggio, S.R., 2014. Electrochemical degradation of a real textile wastewater using β -PbO₂ and DSA® anodes. *Chem. Eng. J.* 251, 138–145. <https://doi.org/10.1016/j.cej.2014.04.032>.
- Asgari, G., Shabanloo, A., Salari, M., Eslami, F., 2020. Sonophotocatalytic treatment of AB113 dye and real textile wastewater using ZnO/persulfate: Modeling by response surface methodology and artificial neural network. *Environ. Res.*, 109367
- Brillas, E., Martínez-Huitle, C.A., 2015. Decontamination of wastewaters containing synthetic organic dyes by electrochemical methods. An updated review. *Appl. Catal. B* 166, 603–643.
- Chen, S., Hu, W., Hong, J., Sandoe, S., 2016. Electrochemical disinfection of simulated ballast water on PbO₂/graphite felt electrode. *Mar. Pollut. Bull.* 105, 319–323.
- Cho, I.-H., Zoh, K.-D., 2007. Photocatalytic degradation of azo dye (Reactive Red 120) in TiO₂/UV system: Optimization and modeling using a response surface methodology (RSM) based on the central composite design. *Dyes Pigm.* 75, 533–543.
- Ciriaco, L., Anjo, C., Correia, J., Pacheco, M., Lopes, A., 2009. Electrochemical degradation of ibuprofen on Ti/Pt/PbO₂ and Si/BDD electrodes. *Electrochim. Acta* 54, 1464–1472.
- Dai, Q., Shen, H., Xia, Y., Chen, F., Wang, J., Chen, J., 2013. The application of a novel Ti/SnO₂-Sb₂O₃/PTFE-La-Ce- β -PbO₂ anode on the degradation of cationic gold yellow X-GL in sono-electrochemical oxidation system. *Sep. Purif. Technol.* 104, 9–16.
- Dai, Q., Zhou, J., Weng, M., Luo, X., Feng, D., Chen, J., 2016. Electrochemical oxidation metronidazole with Co modified PbO₂ electrode: Degradation and mechanism. *Sep. Purif. Technol.* 166, 109–116.
- Dargahi, A., Nematollahi, D., Asgari, G., Shokoohi, R., Ansari, A., Samarghandi, M.R., 2018. Electrodegradation of 2,4-dichlorophenoxyacetic acid herbicide from aqueous solution using three-dimensional electrode reactor with G/ β -PbO₂ anode: Taguchi optimization and degradation mechanism determination. *RSC Adv.* 8, 39256–39268.
- Duan, X., Ma, F., Yuan, Z., Chang, L., Jin, X., 2013. Electrochemical degradation of phenol in aqueous solution using PbO₂ anode. *J. Taiwan Inst. Chem. Eng.* 44, 95–102.
- Garcia-Segura, S., Anotai, J., Singhadech, S., Lu, M.-C., 2017. Enhancement of biodegradability of o-toluidine effluents by electro-assisted photo-Fenton treatment. *Process Saf. Environ. Prot.* 106, 60–67. <https://doi.org/10.1016/j.psep.2016.12.011>.
- Garcia-Segura, S. et al, 2020. Disparities between experimental and environmental conditions: research steps towards making electrochemical water treatment a reality. *Current Opin. Electrochem.*
- Golder, A., Hridaya, N., Samanta, A., Ray, S., 2005. Electrocoagulation of methylene blue and eosin yellowish using mild steel electrodes. *J. Hazard. Mater.* 127, 134–140.
- Gupta, V., 2009. Application of low-cost adsorbents for dye removal—a review. *J. Environ. Manage.* 90, 2313–2342.
- Gupta, V.K., Pathania, D., Agarwal, S., Singh, P., 2012. Adsorptive photocatalytic degradation of methylene blue onto pectin–CuS nanocomposite under solar light. *J. Hazard. Mater.* 243, 179–186.
- Hao, X., Dan, S., Qian, Z., Honghui, Y., Yan, W., 2014. Preparation and characterization of PbO₂ electrodes from electro-deposition solutions with different copper concentration. *RSC Adv.* 4, 25011–25017.
- Jua, L.Y. et al, 2020. Modeling of methylene blue adsorption using functionalized Buckypaper/Polyvinyl alcohol membrane via ant colony optimization. *Environ. Pollut.*, 113940
- Li, X. et al, 2014. High selectivity of benzene electrochemical oxidation to p-benzoquinone on modified PbO₂ electrode. *Appl. Surf. Sci.* 311, 357–361. <https://doi.org/10.1016/j.apsusc.2014.05.068>.
- Li, X., Pletcher, D., Walsh, F.C., 2011. Electrodeposited lead dioxide coatings. *Chem. Soc. Rev.* 40, 3879–3894.
- Li, X., Xu, H., Yan, W., 2016. Preparation and characterization of PbO₂ electrodes modified with polyvinyl alcohol (PVA). *RSC Adv.* 6, 82024–82032.
- Li, X., Xu, H., Yan, W., 2017. Effects of twelve sodium dodecyl sulfate (SDS) on electro-catalytic performance and stability of PbO₂ electrode. *J. Alloys Compd.* 718, 386–395. <https://doi.org/10.1016/j.jallcom.2017.05.147>.
- Lin, H., Niu, J., Xu, J., Li, Y., Pan, Y., 2013. Electrochemical mineralization of sulfamethoxazole by Ti/SnO₂-Sb/Ce-PbO₂ anode: kinetics, reaction pathways, and energy cost evolution. *Electrochim. Acta* 97, 167–174.
- Mandal, P., Gupta, A.K., Dubey, B.K., 2018. A novel approach towards multivariate optimization of graphite/PbO₂ anode synthesis conditions: Insight into its enhanced oxidation ability and physicochemical characteristics. *J. Environ. Chem. Eng.* 6, 4438–4451.
- Mandal, P., Gupta, A.K., Dubey, B.K., 2020. Role of inorganic anions on the performance of landfill leachate treatment by electrochemical oxidation using graphite/PbO₂ electrode. *J. Water Process Eng.* 33. <https://doi.org/10.1016/j.jwpe.2019.101119>.
- Martínez-Huitle, C.A., Panizza, M., 2018. Electrochemical oxidation of organic pollutants for wastewater treatment. *Curr. Opin. Electrochem.* 11, 62–71.
- Martínez-Huitle, C.A., Rodrigo, M.A., Sirés, I., Scialdone, O., 2015. Single and coupled electrochemical processes and reactors for the abatement of organic water pollutants: a critical review. *Chem. Rev.* 115, 13362–13407. <https://doi.org/10.1021/acs.chemrev.5b00361>.
- Nakamura, K.C., Guimarães, L.S., Magdalena, A.G., Angelo, A.C.D., De Andrade, A.R., Garcia-Segura, S., Pipi, A.R.F., 2019. Electrochemically-driven mineralization of Reactive Blue 4 cotton dye: On the role of in situ generated oxidants. *J. Electroanal. Chem.* 840, 415–422. <https://doi.org/10.1016/j.jelechem.2019.04.016>.
- Nasirpour, F., 2017. Electrodeposition of 2D and 3D meso and nanostructures. In: *Electrodeposition of Nanostructured Materials*. Springer, pp. 123–185.
- Neta, P., Huie, R.E., Ross, A.B., 1988. Rate constants for reactions of inorganic radicals in aqueous solution. *J. Phys. Chem. Ref. Data* 17, 1027–1284.
- Neto, S.A., De Andrade, A., 2009. Electrooxidation of glyphosate herbicide at different DSA® compositions: pH, concentration and supporting electrolyte effect. *Electrochim. Acta* 54, 2039–2045.
- Panizza, M., Cerisola, G., 2009. Direct and mediated anodic oxidation of organic pollutants. *Chem. Rev.* 109, 6541–6569.
- Pathania, D., Sharma, S., Singh, P., 2017. Removal of methylene blue by adsorption onto activated carbon developed from Ficus carica bast. *Arab. J. Chem.* 10, S1445–S1451. <https://doi.org/10.1016/j.arabjc.2013.04.021>.
- Paz, A., Carballo, J., Pérez, M.J., Domínguez, J.M., 2017. Biological treatment of model dyes and textile wastewaters. *Chemosphere* 181, 168–177.
- Rahmani, A.R., Godini, K., Nematollahi, D., Azarian, G., 2015. Electrochemical oxidation of activated sludge by using direct and indirect anodic oxidation. *Desalination Water Treat.* 56, 2234–2245.
- Rahmani, A.R., Salari, M., Shabanloo, A., Shabanloo, N., Bajalan, S., Vaziri, Y., 2020. Sono-catalytic activation of persulfate by nZVI-reduced graphene oxide for degradation of nonylphenol in aqueous solution: Process optimization, synergistic effect and degradation pathway. *J. Environ. Chem. Eng.*, 104202 <https://doi.org/10.1016/j.jece.2020.104202>.
- Rahmani, A.R., Shabanloo, A., Fazlzadeh, M., Poureshgh, Y., 2016. Investigation of operational parameters influencing in treatment of dye from water by electro-Fenton process. *Desalination Water Treat.* 57, 24387–24394.

- Rahmani, A.R., Shabanloo, A., Fazlzadeh, M., Poureshgh, Y., Vanaeitabar, M., 2019. Optimization of sonochemical decomposition of ciprofloxacin antibiotic in US/PS/nZVI process by CCD-RSM method. *Desalination Water Treat.* 145, 300–308.
- Rao, A.N.S., Venkatarangiah, V.T., 2014. Metal oxide-coated anodes in wastewater treatment. *Environ. Sci. Pollut. Res.* 21, 3197–3217.
- Ravikumar, K., Deebika, B., Balu, K., 2005. Decolourization of aqueous dye solutions by a novel adsorbent: application of statistical designs and surface plots for the optimization and regression analysis. *J. Hazard. Mater.* 122, 75–83.
- Salari, M., Dehghani, M.H., Azari, A., Motevalli, M.D., Shabanloo, A., Ali, I., 2019. High performance removal of phenol from aqueous solution by magnetic chitosan based on response surface methodology and genetic algorithm. *J. Mol. Liq.* 285, 146–157.
- Samarghandi, M.R., Nemattollahi, D., Asgari, G., Shokoohi, R., Ansari, A., Dargahi, A., 2019. Electrochemical process for 2, 4-D herbicide removal from aqueous solutions using stainless steel 316 and graphite Anodes: optimization using response surface methodology. *Sep. Sci. Technol.* 54, 478–493.
- Samarghandi, M.R., Tari, K., Shabanloo, A., Salari, M., Nasab, H.Z., 2020. Synergistic degradation of acid blue 113 dye in a thermally activated persulfate (TAP)/ZnO-GAC oxidation system: Degradation pathway and application for real textile wastewater. *Sep. Purif. Technol.*, 116931.
- Samet, Y., Elaoud, S.C., Ammar, S., Abdelhedi, R., 2006. Electrochemical degradation of 4-chloroguaiacol for wastewater treatment using PbO₂ anodes. *J. Hazard. Mater.* 138, 614–619. <https://doi.org/10.1016/j.jhazmat.2006.05.100>.
- Seid-Mohammadi, A., Shabanloo, A., Fazlzadeh, M., Poureshgh, Y., 2017. Degradation of acid blue 113 by US/H₂O₂/Fe²⁺ and US/S₂O₈²⁻/Fe²⁺ processes from aqueous solutions. *Desalination Water Treat.* 78, 273–280.
- Shabanloo, A., Salari, M., Shabanloo, N., Dehghani, M.H., Pittman, C.U., Mohan, D., 2020. Heterogeneous persulfate activation by nano-sized Mn₃O₄ to degrade furfural from wastewater. *J. Mol. Liq.* 298. <https://doi.org/10.1016/j.molliq.2019.112088>.
- Shokoohi, R., Bajalan, S., Salari, M., Shabanloo, A., 2019. Thermochemical degradation of furfural by sulfate radicals in aqueous solution: optimization and synergistic effect studies. *Environ. Sci. Pollut. Res.* 26, 8914–8927.
- Shokoohi, R. et al, 2020. Catalytic activation of persulfate with Mn₃O₄ nanoparticles for degradation of acid blue 113: process optimisation and degradation pathway. *Int. J. Environ. Anal. Chem.*, 1–20.
- Shokoohi, R., Shabanloo, A., Vanaei, M., Torkshavand, Z., 2017. Response surface methodological approach for optimizing removal of ciprofloxacin from aqueous solution using thermally activated persulfate/aeration systems. *Global Nest J.* 19, 389–395.
- Sirés, I., Brillas, E., Oturan, M.A., Rodrigo, M.A., Panizza, M., 2014. Electrochemical advanced oxidation processes: today and tomorrow. A review. *Environ. Sci. Pollut. Res.* 21, 8336–8367.
- Soloman, P., Basha, C.A., Velan, M., Balasubramanian, N., Marimuthu, P., 2009. Augmentation of biodegradability of pulp and paper industry wastewater by electrochemical pre-treatment and optimization by RSM. *Sep. Purif. Technol.* 69, 109–117.
- Song, S., Fan, J., He, Z., Zhan, L., Liu, Z., Chen, J., Xu, X., 2010. Electrochemical degradation of azo dye CI Reactive Red 195 by anodic oxidation on Ti/SnO₂-Sb/PbO₂ electrodes. *Electrochim. Acta* 55, 3606–3613.
- Souri, Z., Ansari, A., Nemattollahi, D., Mazloum-Ardakani, M., 2020. Electrochemical degradation of dibenzoazepine drugs by fluorine doped β-PbO₂ electrode: New insight into the electrochemical oxidation and mineralization mechanisms. *J. Electroanal. Chem.*
- Souza, F.L., Aquino, J.M., Irikura, K., Miwa, D.W., Rodrigo, M.A., Motheo, A.J., 2014. Electrochemical degradation of the dimethyl phthalate ester on a fluoride-doped Ti/β-PbO₂ anode. *Chemosphere* 109, 187–194. <https://doi.org/10.1016/j.chemosphere.2014.02.018>.
- Stirling, R., Walker, W.S., Westerhoff, P., Garcia-Segura, S., 2020. Techno-economic analysis to identify key innovations required for electrochemical oxidation as point-of-use treatment systems. *Electrochim. Acta* 338.
- Wang, C., Wang, F., Xu, M., Zhu, C., Fang, W., Wei, Y., 2015. Electrocatalytic degradation of methylene blue on Co doped Ti/TiO₂ nanotube/PbO₂ anodes prepared by pulse electrodeposition. *J. Electroanal. Chem.* 759, 158–166.
- Wang, Y., Shen, C., Li, L., Li, H., Zhang, M., 2016. Electrocatalytic degradation of ibuprofen in aqueous solution by a cobalt-doped modified lead dioxide electrode: influencing factors and energy demand. *RSC Adv.* 6, 30598–30610.
- Wang, Y., Shen, Z., Chen, X., 2010. Effects of experimental parameters on 2, 4-dichlorophenol degradation over Er-chitosan-PbO₂ electrode. *J. Hazard. Mater.* 178, 867–874.
- Wu, F., Li, X., Liu, W., Zhang, S., 2017. Highly enhanced photocatalytic degradation of methylene blue over the indirect all-solid-state Z-scheme g-C₃N₄-RGO-TiO₂ nanoheterojunctions. *Appl. Surf. Sci.* 405, 60–70. <https://doi.org/10.1016/j.apsusc.2017.01.285>.
- Wu, W., Huang, Z.-H., Lim, T.-T., 2014. Recent development of mixed metal oxide anodes for electrochemical oxidation of organic pollutants in water. *Appl. Catal. A Gen.* 480, 58–78.
- Xu, F., Chang, L., Duan, X., Bai, W., Sui, X., Zhao, X., 2019. A novel layer-by-layer CNT/PbO₂ anode for high-efficiency removal of PCP-Na through combining adsorption/electrosorption and electrocatalysis. *Electrochim. Acta* 300, 53–66. <https://doi.org/10.1016/j.jelectacta.2019.01.090>.
- Xu, Z., Yu, Y., Liu, H., Niu, J., 2017. Highly efficient and stable Zr-doped nanocrystalline PbO₂ electrode for mineralization of perfluorooctanoic acid in a sequential treatment system. *Sci. Total Environ.* 579, 1600–1607. <https://doi.org/10.1016/j.scitotenv.2016.11.180>.
- Yang, H., Liang, J., Zhang, L., Liang, Z., 2016. Electrochemical oxidation degradation of methyl orange wastewater by Nb/PbO₂ electrode. *Int. J. Electrochem. Sci.* 11, 1121–1134.
- Yang, K., Liu, Y., Qiao, J., 2017. Electrodeposition preparation of Ce-doped Ti/SnO₂-Sb electrodes by using selected addition agents for efficient electrocatalytic oxidation of methylene blue in water. *Sep. Purif. Technol.* 189, 459–466.
- Yao, X. et al, 2020. Magnetic activated biochar nanocomposites derived from wakame and its application in methylene blue adsorption. *Bioresour. Technol.* 302.
- Yao, Y., Huang, C., Yang, Y., Li, M., Ren, B., 2018. Electrochemical removal of thiamethoxam using three-dimensional porous PbO₂-CeO₂ composite electrode: Electrode characterization, operational parameters optimization and degradation pathways. *Chem. Eng. J.* 350, 960–970.
- Yao, Y., Li, M., Yang, Y., Cui, L., Guo, L., 2019. Electrochemical degradation of insecticide hexazinone with Bi-doped PbO₂ electrode: Influencing factors, intermediates and degradation mechanism. *Chemosphere* 216, 812–822.
- Yao, Y., Ren, B., Yang, Y., Huang, C., Li, M., 2019. Preparation and electrochemical treatment application of Ce-PbO₂/ZrO₂ composite electrode in the degradation of acridine orange by electrochemical advanced oxidation process. *J. Hazard. Mater.* 361, 141–151.
- Zhang, J., Lee, K.-H., Cui, L., Jeong, T.-S., 2009. Degradation of methylene blue in aqueous solution by ozone-based processes. *J. Ind. Eng. Chem.* 15, 185–189.
- Zhao, Q., Wei, F., Zhang, L., Yang, Y., Lv, S., Yao, Y., 2019. Electrochemical oxidation treatment of coal tar wastewater with lead dioxide anodes. *Water Sci. Technol.* <https://doi.org/10.2166/wst.2019.323>.